International Journal of Signal Processing, Image Processing and Pattern Recognition
Vol.9, No.3 (2016), pp.247-260
http://dx.doi.org/10.14257/ijsip.2016.9.3.22

A Novel Time of Arrival Estimation Algorithm based on Skewness and Kurtosis

Xiaolin Liang[1], Hao Zhang[1, 2], Tingting Lv[1] and T. Aaron Gulliver[2]

[1]*College of Information Science and Engineering, Ocean University of China*
Qingdao, 266100, China
[2]*Department of Electrical and Computer Engineering, University of Victoria*
Victoria, bV8W 3P6, Canada
xiaolin87liang@163.com,zhanghao@ouc.edu.cn
lvtingting33@163.com,agullive@ece.uvic.ca

Abstract

Impulse radio60GHz signalsaremuch more practical for ranging and localizationsystemswith high time and multipath resolution.In order to improve the precision ofTOA estimation, a new TOA estimation algorithm based on energy detector(ED) is proposed whichbased on a joint metric of the skewnessand kurtosisafter ED. Thethreshold based on the signal-to-noise ratio (SNR) isinvestigated. Simulation resultsshowforIEEE802.15.3c channel models, the proposed algorithmprovides better precisionthan other ED-based algorithms.

Keywords*: 60GHz, TOA estimation, energy detector, skewness, kurtosis*

1. Introduction

The demand for high data rate wireless communications with low latency has increased dramatically in recent years. Unfortunately, due to spectrum limitations and transmit power regulations, current short-range wireless communication strategies cannot achieve Gigabit per second (Gbps) data rates. Fortunately, wireless communications in the 60GHz millimeter wave (mm-wave) band has become viable for Gbps wireless communication networks [1-4] due to the availability of several GHz of license-free spectrum, up to 10W maximum transmit power, no interference from other systems, and the development of low-cost complementary metal-oxide semiconductordevices. The federal communications commissionpermits communications in the 60GHz unlicensed band at an effective isotropic radiated power (EIRP) of up to 40dBm, which is many times greater than other short-rangewireless communication strategies. In China, this limit is 44dBm [5]. Although the path lossis high at 60GHz, the received power can still be significant. Impulse radiocommunication strategies have been proposed for this frequency band because it can be effective in separating the multipath signals at the receiver. This is because short pulses are employed for communications with a duration (typically under 100 picoseconds), which is far less than the multipath propagation delay. These signals can also provide the fine multipath resolution required for high precision ranging and localization [6]. Thus, 60GHz signals are even much suitable for localization applications for short distances.

Generally, the localizationstrategies can be classified into range based[7-10] and non-range based [11]. For example, TOA [10, 12] and Time Difference of Arrival (TDOA) [10] are range based strategies, while Received Signal Strength (RSS) and Angle of Arrival(AOA) [11] are non-range based. Localization that based on range (TOA or TDOA) is even much suitable for usingwithIR-60GHzstrategy [11], as it can take full advantage of the higher time and multipath resolution available with very short IR-60GHzsignals. TOA estimation which is even much more accurate is the key to accurate ranging, but this is very challenging due to the potentially hundreds of multipath components in 60GHz channels, even in the Non-line of

ISSN: 2005-4254 IJSIP

Sight (NLOS) environments.TOA estimation has been extensively studied [12, 15-18] forpast few years. There are two approaches which are much more applicable forTOA estimation,Matched Filter (MF) [16] (such as a rake or correlation receiver) with a higher sampling rate and higher precision correlation, or an ED[18] with a lower sampling rate and lower complex.MFis the optimal strategy for TOA estimation, where a correlator template is matched exactly to the received signal. However, a receiver operating at the Nyquist sampling rate makes it very difficult to align with the multipath components of the received signal [15].

Inaddition,MFrequires a priori estimation of the channel, including the timing, fading coefficient, and pulse shape for each component of the impulse response [15]. Because of the higher sampling rates and channel estimation,MFmay not be practical in many applications. As opposed toMF,EDis a non-coherent approach to TOA estimation. It consists of a square-law device, followed by an integrator, sampler and a decision mechanism. The TOA estimate is made by comparing the integrator output with a threshold and choosing the first sample to exceed the threshold. This is a convenient strategy that directly yields an estimate of the start of the received signal. Thus, a lowcomplexity, low sampling rate receiver can be employedwithout the need for a priori channel estimation.The major challenge with EDis the selection of anappropriate threshold based on the received signalsamples.

In this paper, we consider the relationship between theSNR and the statistics of the integrator output includingkurtosis and skewness. A metric based on kurtosis and skewness is then developed for threshold selection. Thethreshold for different SNR values is investigated and theeffects of the integration period and channel areexamined. Performance results are presented which showthat in both the CM1.1 and CM2.1 channels, this joint metricprovides higher precision and robustness.

The remainder of this paper is organized as follows. InSection 2 the system model is outlined. Section 3discusses various TOA estimation algorithms based onED. Section 4 considers the statisticalcharacteristics of the energy values. In Section 5 a jointmetric based on kurtosis and skewnessisproposed.Some performanceresults are presented in section 6 and section 7 concludes the paper.

2. System Model

Currently, there are two important standards that have been developed for 60GHz wirelesscommunications systems, IEEE 802.15.3c and IEEE 802.11ad [19-20]. In this paper, the channel models in IEEE 802.15. 3c standard are used because it is specifically designed for Wireless Personal Area Networksand thus encompasses typical indoor environments. Further, these are the most widely employed models for 60GHz systems. IEEE 802.15.3c standard was the first developed for high data rate short-range wireless systems. The physical layer was designed to support the transmission of data within a few meters at a minimum data rate of 2Gbps. These models have been developed for communications in the frequency band 57 to 66GHz in indoor residential, indoor office and library environments (with differences largely due to the LOS and NLOS characteristics) [21-25]. In this paper, a pulse position modulation time hopping60GHz signal is employed for ranging purposes. The propagation delay $\hat{\tau}$, between the transmitter and receiver is estimated for use in localization.

2.1. 60GHz Signal

The 2PPM-TH-60GHz signals have a very short duration (typically 100 picoseconds or less), and can be expressed as:

$$s(t)=\sum_{-\infty}^{\infty} p\left(t-jT_s-C_jT_c-a_j\varepsilon\right) \quad (1)$$

where T_s is the symbol time. The Time Hoppingcode represented by C is a pseudorandom integer-valued sequence which is unique for each user to limit multiple access interference, and T_c is the chip time. The PPM time shift is ε so that if a_j is 1, the signal is shifted in time by

ε , while a_j is 0, there is no shift. In general, these parameters satisfy the following relationship $C_j T_c + \varepsilon < T_s ; \varepsilon < T_c ; a_j \varepsilon < C_j T_c (C_j \neq 0)$ Many pulse shapes have been proposed for 60 GHz systems. In this paper a Gaussian pulse is employed which is multiplied by the carrier signal to give as shown in the Figure1 [26]:

$$p(t) = \frac{\sqrt{2}}{\alpha} \exp\left(-2\pi \frac{t^2}{\alpha^2}\right) \cos(2\pi f_c t) \quad (2)$$

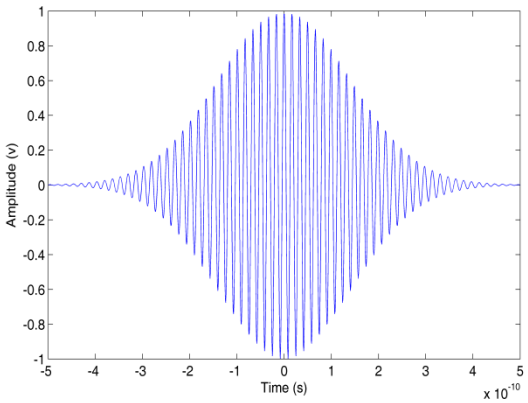

Figure 1. Waveform of the 60GHz Signal

where α is the shape factor, and f_c is the carrier frequency which here is $f_c = 60$ GHz. A smaller shape factor results in a shorter duration pulse and a larger bandwidth.

2.2. Signal Shift and Path Loss

The path loss is defined as the ratio of the received signal power to the transmit signal power and it is very important for link budget analysis. Unlike narrow-band system, the path loss for a wide-band system such asmm-wave systemis both distance and frequency dependent. In order to simplify the models, it is assumed that the frequency dependence path loss is negligible and only distance dependence path loss is modeled. The signal path loss, which depends on the propagation distance and the channel (IEEE802.15.3c), is described by

$$PL(d)[dB] = PL_0 + 10 \cdot n \log_{10}\left(\frac{d}{d_0}\right) + X_\sigma [dB]; \; d \geq d_0 \quad (3)$$

where d_0 and d denote the reference distance, and distance respectively. Thepath loss exponent n for mm-wave based measurements ranges from 1.2-2.0 for LOS and from 1.97-10 for NLOS, in various different indoor environments. In the presence of wave guiding effects and reverberation effects which lead to increase in power levels by multipath aggregation, n can be smaller than 2. X_σ is that the unit dB, with mean zero and variance σ_s for a Gaussian random variable [11]. Table 1 summarizes the values of n, PL_0 , σ_s for different environments and scenarios.

Table1.Values of *n* PL_0 σ_s for Different Environments and Scenarios

environments	n	PL_0	σ_s
Indoorresidential(LOS)	1.53	75.1	1.50
indoor residential(NLOS)	2.44	86.0	6.20
indoor office (LOS)	1.16	84.6	5.40
indoor office (NLOS)	3.74	56.1	8.60

The signal shift can be expressed as:

$$t = dt * floor\left(\left(d / c\right)/dt\right) \quad (4)$$

where*d* denote the distance between the transmitter and receiver, *dt* is the sampling period and *c* is the speed of light which is 299792458m/s in the air.

2.3. Multipath Fading Channel

The received signal can be written as:

$$r(t) = \sum_{n=1}^{N} \alpha_n p(t - \tau_n) + n(t) \quad (5)$$

where*N* is the number of received multipath components, α_n and τ_n denote the amplitude and delay of the nth path respectively, *p*(*t*) is the received 60GHz pulse and *n*(*t*) isAWGNwith zero meanand twosidedpower spectral density $N_0/2$. Equation (5)can be rewritten as:

$$r(t) = s(t) * h(t) + n(t) \quad (6)$$

where $s(t)$ is the transmitted signal, and $h(t)$ is the channel impulse response which can be expressed as:

$$h(t,\theta) = \sum_{k=1}^{K} \sum_{l=1}^{L_k} \mu_{kl} \delta(t - T_k - \tau_{kl}) \delta(\theta - \theta_k - \omega_{kl}) \quad (7)$$

where $\delta(.)$ is the diracdelta function, K is the number of clusters, L_k is the number of rays in the k^{th} cluster, and μ_{kl} , τ_{kl} and ω_{kl} denote the complex amplitude, delay and azimuth of the k^{th} ray of the l^{th} cluster, respectively. Similarly, T_k and θ_k represent the delay and mean AOAof the k^{th} cluster.

2.4. Energy Detector

As shown in Figure 2 [27], after the amplifier, the received signals are squared, and then input to an integrator with integration period Tb. Because of the inter-frame leakage due to multipath signals, the integration duration is $3T_f / 2$, so the number of signal values for Energy Detector is $N = 3T_f / 2Tb$. The integrator outputs can be expressed as:

$$z[n] = \sum_{i=1}^{N} \int_{(i-1)T_f + (c_j + n)Tb}^{(i-1)T_f + (c_j + n - 1)Tb} r^2(t) dt \quad (8)$$

where $n \in \{1, 2, .., N\}$ denotes the sample index with respect to the starting point of the integration period and *N* is the number of pulses per symbol. Here, *N* is set to 1,so the integrator outputs are:

$$z[n] = \sum_{i=1}^{N} \int_{(c_j + n)Tb}^{(c_j + n - 1)Tb} r^2(t) dt \quad (9)$$

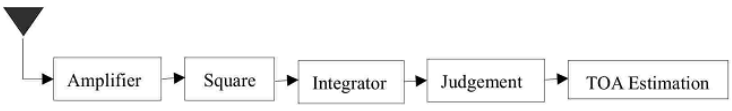

Figure 2. Block Diagram of the Energy Detector Receiver

If $z[n]$ is the integration of noise only, it has a centralized Chi-square distribution, while it has a non-centralized Chi-square distribution if a signal is present.The mean and variance of the noise and signal values are given by [17] respectively.

$$\mu_0 = F\sigma^2, \sigma_0 = 2F\sigma^4 \quad (10)$$

$$\mu_e = F\sigma^2 + E_n, \sigma_e^2 = 2F\sigma^4 + 4\sigma^2 E_n \quad (11)$$

where E_n is the signal energy within the *nth*integration period and F is the number of degrees offreedom given by $F = 2BTb + 1$. Here B is the signalbandwidth.

3. TOA Estimation Based on Energy Detector

3.1. TOA Estimation Algorithms

There are many TOA estimation algorithms based on EDfor determining the start block of a received signal. The simplest is Maximum Energy Selection (MES), which chooses the maximum energy valueto be the start of the signal value. The TOA is estimated as the center of the corresponding integration period

$$\tau_{MES} = \left[\arg\max_{1 \le n \le N_b} \{ z[n] \} - 0.5 \right] Tb \quad (12)$$

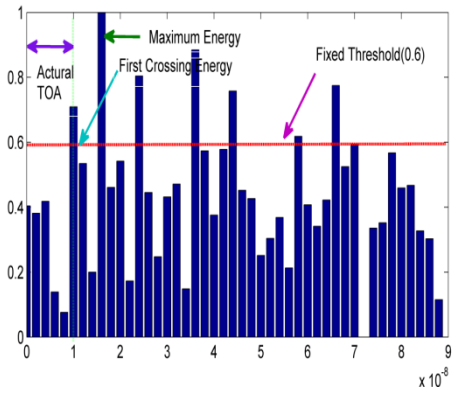

Figure3. TOA Estimation Based on Energy Detector

However, as show inFigure 3, the maximum energy value may not be the first energyblock [13], especially in NLOS environments. On average, the first energy value $z[n]$ islocated before the maximum $z[n_{\max}]$, i.e. $n \le n_{\max}$. Thus,Threshold CrossingTOA estimation has beenproposed where the received energy values are comparedto an appropriate threshold α. In this case, the TOAestimation is given by

$$\tau_{TC} = \left[\arg\min_{1 \le n \le n_{\max}} \{ n \mid z[n] \ge \xi \} - 0.5 \right] Tb \quad (13)$$

It is difficult to determine an appropriate threshold α directly, so usually a normalized threshold α_{norm} is calculated. Using α_{norm}, α is given by

$$\alpha = \alpha_{norm} \left(\max\left(z(n)\right) - \min\left(z(n)\right) \right) + \min\left(z(n)\right) \quad (14)$$

The TOAis then obtained using (11).A simpler Threshold Crossing algorithm is the FixedThresholdalgorithm where the threshold is set to a fixed value, forexample α_{norm}=0.4 .The problem in this case becomes one of how to set the threshold. It should be based on the statistics of the signal energy, particularly for multipath, NLOS indoor environments.

3.2. Error Analysis

The Mean Absolute Error (MAE) of TOA estimation based on Threshold Crossingwas analyzed, and closed form error expressions derived. The MAE can be used to evaluate the

quality of an algorithm, and is defined as:

$$MAE = \frac{1}{N}\sum_{n=1}^{N}\left(t_n - t_n\right) \quad (15)$$

where t_n is the *nth* actual propagation time, t_n is the *nth* TOA estimate, and *N* is the number of TOA estimates.

4. Statistical Characteristics

Kurtosis and skewnessof the energy blocks are analyzed in this section.

4.1. Kurtosis

The kurtosisis calculated using the second and fourth order moments and is given by:

$$k = \frac{E\left[\left(x_i - \mu_x\right)^4\right]}{E\left[\left(x_i - \mu_x\right)^2\right]^2} = \frac{E\left[\left(x_i - \mu_x\right)^4\right]}{\sigma_x^4} \quad (16)$$

where μ_x is the mean value, and σ_x is the standard deviation. The kurtosis for a standard normal distribution is three. For this reason, kurtosis is often redefined as $\mathrm{K} = \mathrm{K} - 3$ (often referred to as "excesskurtosis"), so that the standard normal distribution has a kurtosis of zero, positive kurtosis indicates a "peaked" distribution and negative kurtosisindicates a "flat" distribution. For noise only (or for a low SNR) and sufficiently large *F* (degrees of freedom of the Chi-square distribution), $z[n]$ has a Gaussian distribution and kurtosis =0. On the other hand, as the SNR increases, kurtosis will tend to increase.

4.2. Skewness

The skewness is given by:

$$S = \frac{1}{\left(N-1\right)\delta^3}\sum_{i=1}^{N}\left(x_i - \mu_x\right)^3 \quad (17)$$

where μ_x is the mean value, and δ is the standard deviation ofthe energy values. The skewness for a normal distributionis 0, in fact any symmetric data will have a skewnessof zero. Negative values of skewness indicate that thedata is skewed left, while positive values indicate datathat is skewed right. Skewed left indicates that the left tailis long relative to the right tail, while skewed rightindicates the opposite. For noise only (or very low SNR),and sufficiently large *F*, skewness≈0. As the SNR increases, skewnesswill tend to increase.

4.3. Characteristics ofParameters

In order to examine the characteristics of parameters, the CM1.1 (residential LOS) and CM2.1 (residential NLOS) channel models from the IEEE802.15.3c standard are employed. For eachSNRvalue, 1000 channel realizations are generated and sampled at $f_c = 1 \cdot e^{10}$ Hz. The other system parameters are $T_f = 200ns$, $T_c = 1ns$, the value of Tb is from1ns to 4nsand N=1. Each realization has a TOA uniformly distributed within $\left(0\, T_f\right)$ .The parameters were calculated, and the results obtained are shown in from Figures 4-5. This results show that the characteristics of the parameters with respect to the SNR are similar for the two channels. The results ofthe divisionof two variables (kurtosis and skewness)used as the new parameter 'S/K'. By the same token, the results of the divisionof two variables (kurtosis and skewness) are used as the new parameter 'K/S'.

From Figures 4-5, results showthat K/S, skewness, kurtosis increases as the SNR increases both inchannel CM1.1 and CM2.1, but K/S changes more rapidly in comparison with otherparameters. Conversely, the S/K decrease with the increaseof the SNR. They better

reflectchanges in SNR, and so they are even more suitable for TOA estimation. Moreover,when the SNR is less than 12dB, K/S changes slowly while the SM changes rapidly.On the other hand, when the SNR is higher than 12dB, the S/K changes rapidlybut the K/S changes slowly. Therefore, no single parameter is a good measure ofSNR change over a wide range of values. Thus, a joint metric based on Skewness and Kurtosisis proposed in the next sectionfor TOA estimation.Based on the results in Section 4.5, a joint metric for TOA estimation is formulated as:

$$G = K / S - S / K \quad (18)$$

where 'K/S' is the results of the division of two variables (kurtosis and skewness)and 'S/K' is the results of the division of two variables (kurtosis and skewness).

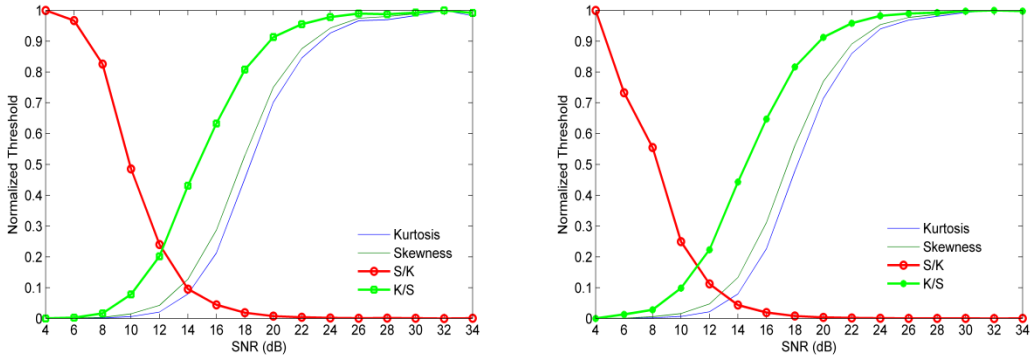

Tb=1ns Tb=4ns

Figure 4. Parameters Change with SNR in CM1.1

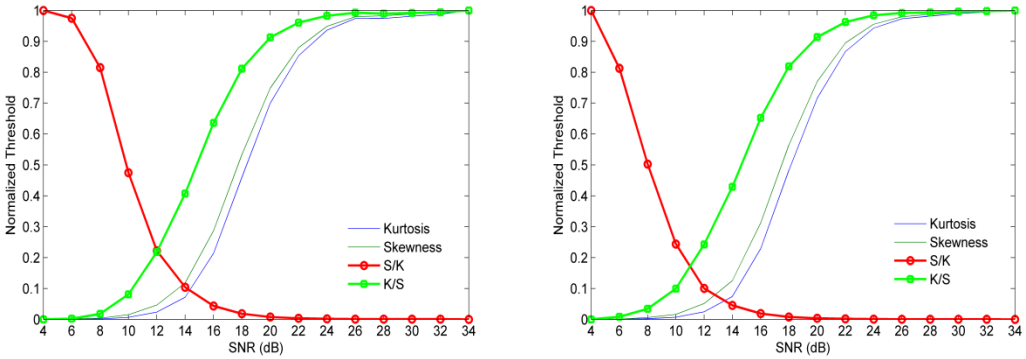

Tb=1ns Tb=4ns

Figure 5. Parameters Change with SNR in CM2.1

5. Optimal Threshold Selection

The relationship between G and the optimal normalized threshold α_{opt} must beestablished. According to Figure 6, the curves forCM1.1 andCM2.1 for a given value of*Tb* are similar, so models are derived only for *Tb*=1nsand4ns.The steps to establish therelationship between G and α_{opt} can expressed as:(1)Generating amounts of channel realizations (1000 channel realizations are generated in this paper)aiming at different channel model (CM1.1 and CM2.1), *Tb*=1nsand 4ns, and SNRvalue in the range from 4to 34dB.(2) Calculating the average value of MAEwith respect to different α_{norm} for different*G*value,channel model(CM1.1 and CM2.1), and *Tb* as shown insection"Relationship between MAE and the Normalized Threshold". In the process of simulation, becauseof the signals are generated randomly, so there are different

MAE valueswith respect to one normalized threshold, so theaverage MAE is obtained. At the sametime, because *G* is a real value, G should be roundedto the nearest discrete value, for example integervalue or half-integer value.(3) Selecting the normalized threshold with the lowestMAE as the best threshold α_{best} with respect to G for each channel model and *Tb*, asshown in Section "Optimal thresholds".(4) Calculating the average normalized thresholds ofchannels CM1.1 and CM2.1 for differentG as the optimalnormalized threshold α_{norm} , as shown in Section"Optimal thresholds".

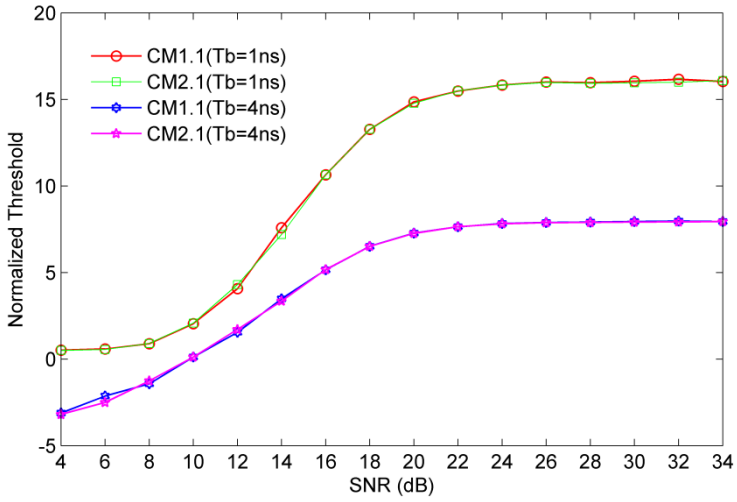

Figure 6. Average Values with Respect to SNR

5.1. Relationship between G and SNR

In order to verify the relationship between the proposed metric G and SNR, 1000 channel realizationswere generated when SNR is from 4to 34 dB in eachIEEE802.15.3c channel. The average values of G arepresented in the Figure 6. The results showG is a monotonicfunction for a large range of SNR values, andit is even much more sensitive tochanges in SNR. The eight fixed curves differ somewhat due to thechannel model and integration period used. The figureshows that G is more sensitive to *Tb* .

5.2. Relationship between MAE and the Normalized Threshold

In order to determine the best threshold (α_{best}) based onG, the relationship between MAE and normalizedthreshold (α_{norm}) was investigated. 1000 channel realizations with SNR={4, 5,⋯, 34} dB weresimulated under CM1.1 and CM2.1 environments α is the threshold which is compared to theenergy values to find the first threshold crossing. When α is bigger than $z[n_{\max}]$, we can't get the TOA estimation, so in this case, α is setto be 1.In the simulation, all G values were rounded to thenearest integer and half-integer values for all SNRvalues.From Figures7-8showthe relationship between MAE and the Normalized Thresholdin the CM1.1 and CM2.1channels, respectively, with *Tb* is1ns. Therelationship is always that the MAE decreases as Gincreases. Another conclusion is that the minimum MAEis lower as Gincreases. The normalized threshold α_{norm} with respect to the minimum MAE is just the bestthreshold α_{best} . The relationship between α_{best} and Gwill be shown in the next Section.

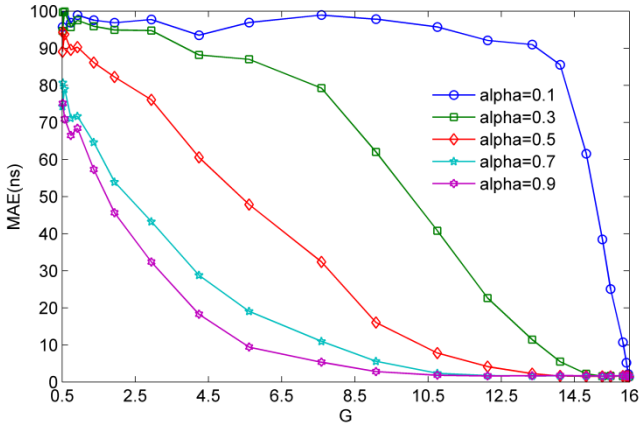

Figure7.MAE with Respect to G (CM1.1)

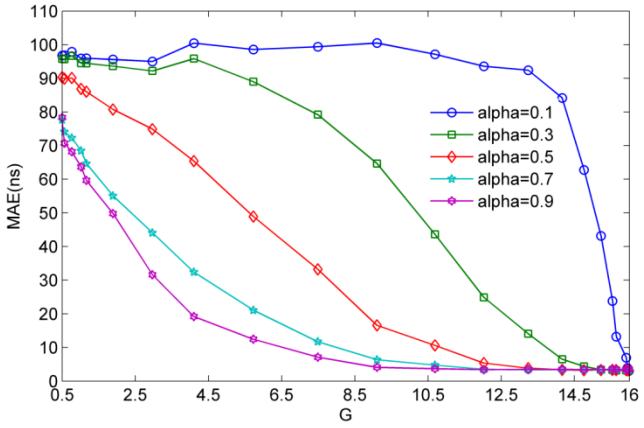

Figure 8.MAE with Respect to G(CM2.1)

5.3. Optimal Thresholds

The normalized threshold α_{norm} with respect to the minimum MAE is called the best threshold α_{best} for a given G. Therefore, the lowest points of the curves in Figures 7-8for each G are selected as the α_{best} . These results show that the relationship between the two parameters is not affected significantly by the channel model, but is more dependent on the integration period, so the values for channels CM1.1 and CM2.1 can be combined. Therefore, the average of the two values is used as the optimal normalized threshold

$$\alpha_{opt}^{(Tb=1ns)}(G)=\frac{\alpha_{best}^{(CM1.1,\,Tb=1ns)}(G)+\alpha_{best}^{(CM2.1,\,Tb=1ns)}(G)}{2} \quad (19)$$

$$\alpha_{opt}^{(Tb=4ns)}(G)=\frac{\alpha_{best}^{(CM1.1,\,Tb=4ns)}(G)+\alpha_{best}^{(CM2.1,\,Tb=4ns)}(G)}{2} \quad (20)$$

5.4. Normalized Threshold with G

From the results in the previous section, the relationship between α_{best} and G shows in Figure9 (1ns) and Figure 10 (4ns) for each value of G. This shows that the relationship between thetwo parameters is not affected significantly by the CM, but is more dependent on theintegrationperiod. Therefore, four piecewise functions were fitted totheseresults aiming at

$Tb=(1ns,4ns)$. The relationship can be described as expression (21), expression (22).

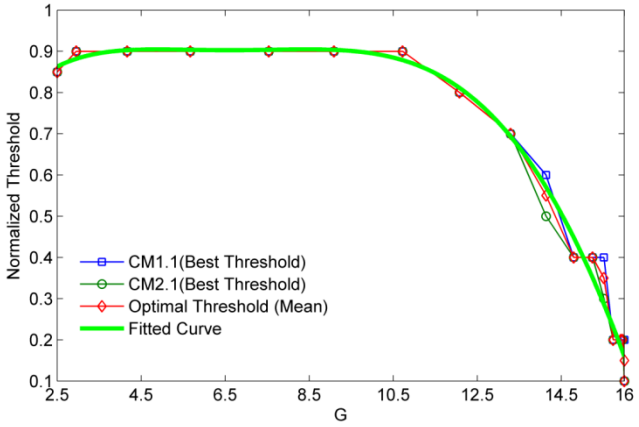

Figure 9. Normalized Threshold with Respect to GTb=1ns

$$\alpha_{best}=\begin{cases}0.8 & x<2.5\\ 7.906e^{-6}x^5-4.421e^{-4}x^4+8.214e^{-3}x^3-0.06866x^2+ & \\ 0.2663x+0.5144 & 2.5\le x<16\\ 0.1 & 16\le x\end{cases} \quad (21)$$

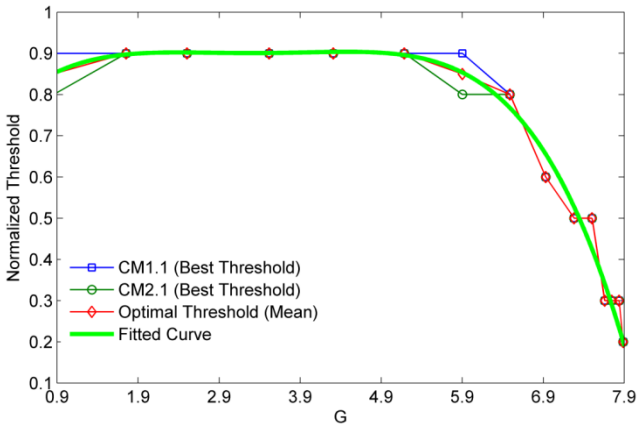

Figure 10. Normalized Threshold with Respect to GTb=4ns

$$\xi_{best}=\begin{cases}0.8 & x<0.9\\ -2.139e^{-5}x^5-1.474e^{-3}x^4+0.02248x^3- & \\ 0.1146x^2+0.2465x+0.7105 & 0.9\le x<7.9094\\ 0.1 & 7.9094\le x\end{cases} \quad (22)$$

6. Results and Discussion

In this section, the MAE is examined for different TOA estimation algorithms which based on EDinIEEE 802.15.3cchannels. As before, 1000 channelrealizations are generated for each case. A 2PPM-TH-60GHz signal isemployed, and the received signal is sampled at $f_c=1\cdot e^{10}$ Hz.The other system parameters are $T_f=200ns$, $T_c=1ns$ Tb is 1ns and 4ns and N=1. Each realization has a TOA uniformly distributed within (0-T_f).The MAE for SNRvalues from 4to

34dB in LOSis presented in the Figure11($Tb = 1ns$ *and* $4ns$). At the same time, The MAE for SNRvalues from 4to 34dB in NLOSis presented in the Figure 12($Tb = 1ns$ *and* $4ns$). This shows that theproposed algorithm performs even much better than other algorithm such as MES and Fixed Threshold. Theperformance in CM1.1 is better than in CM2.1 aiming at the same Tb . In most cases, the performance with $Tb = 1ns$ is better than that with $Tb = 4ns$ regardless of the channel.The MAE performance withthree TOA algorithms in channels CM1.1 and CM2.1 are shown in Figures 11-12respectively.

Here "MES"is the maximum energy selectionalgorithm, and the normalized threshold for the fixedthreshold algorithm is set to 0.4 and 0.6. The MAE with the proposedalgorithm is lower thanother algorithms,particularly at low to moderate SNR values. Theproposed algorithm is better except when the SNR isgreater than 19dB. The performance of the proposed algorithm is morerobust than the other algorithms, as the performancedifference is very smallcompared to the difference with other algorithms.For almost all SNR values the proposed algorithm is even much better. Conversely, the performance of other algorithmsvaries greatlyand is very bad for low to moderate SNRvalues.

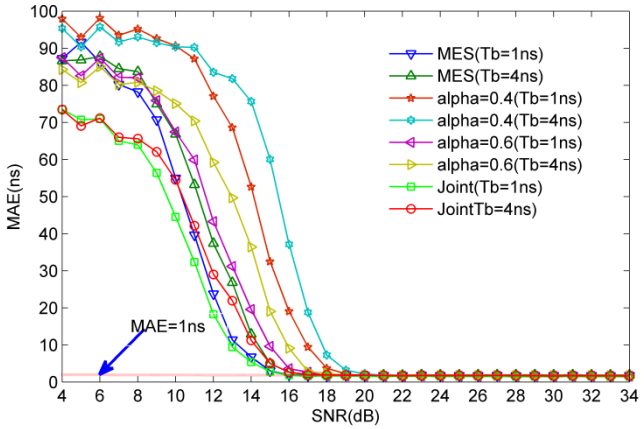

Figure 11. MAE for Different Algorithms with CM1.1 (*Tb*=1ns and 4ns)

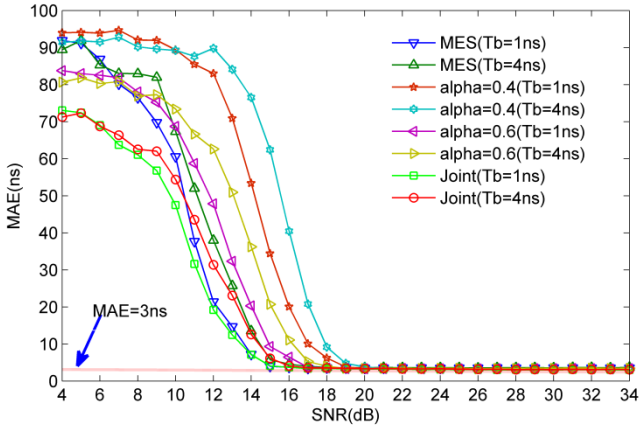

Figure 12. MAE for Different Algorithms with CM2.1 (*Tb*=1ns and 4ns)

7. Conclusion

Low complexTOA estimationalgorithms that based on EDhave been examined for60GHz ranging and positioningapplications. Statisticalparameters were investigated and a joint metric based on skewness and kurtosis was developed for TCTOAestimation according to the resultsobtained. The best normalized threshold wasdetermined using simulation with the

CM1.1 and CM2.1 channels. The effects of the integrationperiod and channel model were investigated. It wasdetermined that the proposed threshold selectiontechnique is largely independent of the channel model.The performance of the proposed algorithm was shown tobe better than several known algorithms. In addition, theproposed algorithm is more robust to changes in the SNRand integration period.

Acknowledgments

The authors would like to thank colleagues from the UWB Laboratory in the College of Information Science and Engineering, Ocean University of China, for help with obtaining the measurement data. This work was supported by the Nature Science Foundation of China under Grant No. 60902005, the Qingdao International Science and Technology Cooperation Projects of Qingdao under Grant No. 12-1-4-137-hz, and the Qingdao Transformation of Scientific and Technological Achievements Guiding Plan (youth special program) under Grant No. 14-2-4-37-jch.

References

[1] L. Zhang, "A fully integrated 60GHz five channel CMOS receiver with 7GHz ultra-wide band width for IEEE 802.11ad standard", Communication, China, vol. 11, no. 6, **(2014)**, pp. 42-50.
[2] S. K. Yong and C. C. Chong, "An overview of multigigabit wireless through millimeter Wave Strategy: Potentials and Technical Challenges", EURASIP J. Wireless Communications and Networking, vol. 2007, no. 1, **(2007)**, pp. 1-10.
[3] R. C. Daniels and R. W. Heath, "60 GHz wireless communications: emerging requirements and design recommendations", IEEE Vehicular Strategy Society, vol. 2, **(2007)**, pp. 41-50.
[4] C. C. Chong, F. M. Peter, Smulders, et al, "60GHz-Millimeter-Wave Radio Principle, Strategy, and News Results", EURASIP Journal on Wireless Communications and Networking, vol. 2007, no. 1, **(2007)**, pp. 1-8.
[5] S. K. Yong, P. F. Xia P F and Alberto V G, "60-GHz Strategy for Gbps WLAN and WPAN: From Theory to Practice", Beijing: Press of China Machine, **(2013)**.
[6] R. C. Daniels and R. W. Health, "60 GHz wireless communications: emerging requirements and design recommendations", IEEE Vehicular Strategy Magazine, vol. 2, no. 3, **(2007)**, pp. 41-50.
[7] D. Jie, X. Cui, H. Zhang, and G. Wang, "A ultra-wideband location algorithm based on neural network". International Conference on WirelessCommunications Networking and Mobile Computing (WiCOM), vol. 11, no. 6, (**2010)**, pp. 56-64.
[8] X. Tu, H. Zhang, X. Cui and T. A. Gulliver, "3D TDOA/AOA location based on extended Kalman filter", International Symposium on Antennas, Propagation and EM Theory (ISAPE), vol. 11, no. 6, (**2010)**, pp. 56-64.
[9] Z. Sahinoglu and S. Gezici, "Ranging in the IEEE 802.15.4a standard", in IEEE Wireless and Microwave Strategy Conference (WAMICON), **(2006)**.
[10] D. Dardari, A. Conti, U. Ferner, A. Giorgetti, and M. Z. Win, "Ranging with ultra-wide bandwidth signals in multipath environments", Proceedings of the IEEE, vol. 97, no. 2, (**2009)**, pp. 404-426.
[11] Y. Zhang, A. K. Brown, W. Q. Malik, and D. J. Edwards, "High resolution 3D angle of arrival determination for indoor UWB multipath propagation", Transactions on Wireless Communications, vol. 7, no. 8, (**2010)**, pp. 3047-3055.
[12] D. Dardari, A. Giorgetti, and M.Z. Win. "Time of arrival estimation of UWB signals in the presence of narrowband and wideband interference", IEEE International Conference on Ultra-Wideband (ICUWB), **(2007)**.
[13] M. Bocquet, C. Loyez, and A. BenlarbiDelai, "Using enhanced TDOA measurement for indoor localization", IEEE Microwave and WireleSG Components Letters, vol. 15, no.10, (**2005)**, pp. 612-614.
[14] A. Abbasi and M.H. Kahaei, "Improving source localization in LOS and NLOS multipath environments for UWB signals". International CSI Computer Conference, **(2009)**.
[15] I. Guvenc and Z. Sahinoglu, "Multi-scale energy products for TOA estimation in IRUWB systems",IEEE Global Telecommunications Conference, (GLOBECOM), **(2005)**.
[16] A. Y.Z. Xu, E. K. S. Au, A. K.S. Wong, and Q. Wang, "A novel threshold based coherent TOA estimation for IR-UWB systems", IEEE Transactions on Vehicular Strategy, vol. 58, no. 8, **(2009)**, pp. 4675-4681.
[17] I. Guvenc and Z. Sahinoglu, "Threshold selection for UWB TOA estimation based on kurtosis analysis", IEEE Communications Letters, vol. 9, no. 12, **(2005)**, pp. 1025-1027.
[18] I. Guvenc and Z. Sahinoglu. "Threshold based TOA estimation for impulse radio UWB systems", IEEE International Conference on Ultra-Wideband,**(2005)**.
[19] "IEEE Standard for Information strategy--Local and metropolitan area networks--Specific requirements--Part 15.3: Wireless Medium Access Control (MAC) and Physical Layer (PHY) Specifications for High Rate Wireless Personal Area Networks (WPAN) amendment 2:millimeter-wave-based alternative physical layer extension". IEEE Computer Society, New York, USA, **(2009)**
[20] "802.11n-2009-IEEE Standard for Information strategy-- Local and metropolitan area networks--Specific

requirements--Part 11: Wireless LAN Medium Access Control (MAC)and Physical Layer (PHY) Specifications Amendment 5: Enhancements for Higher Throughput", IEEE Computer Society, IEEE 978-0-7381-6731-2. New York, USA, **(2009)**.
[21] C. R. Andersonn and T. S. Rappaport, "In-building wideband partition loss measurements at 2.5 and 60GHz", IEEE Transactions on Wireless Communications, vol. 3, no. 3, **(2004)**, pp. 922-928.
[22] S. Collong, G. Zaharia and G. E. Zein, "Influence of the human activity on wide-band characteristics of the 60GHz indoor radio channel", IEEE Transactions on Wireless Communications, vol. 3, no. 6, **(2005)**, pp. 2396-2406
[23] A. Maltsev, R. Maslennikov and A. Sevastyanov, "Experimental investigations of 60GHz WLAN systems in office environment", IEEE Journal on Selected Areas in Communications, vol. 27, no. 8, **(2009)**, pp. 1488-1499.
[24] M. G. Sanchez, A. V. Alejos and I. Cuinas,"Comparision of space diversity performance in indoor radio channels at 40GHz and 60GHz", Proc. of European Conference on WirelessStrategy, Amsterdam, **(2008).**
[25] H. B. Yang,"Channel characteristics and transmission performance for various channel configurations at 60GHz", EURASIP Journal on Wireless Communications and Networking, vol. 2007, no. 1, **(2007)**.
[26] N. Li, "Study on the properties of 60 GHz impulse radio communication system". Qingdao: Ocean University of China, **(2012)**.
[27] X. Cui, C. Wu and J. Li, "UWB simulation of energy detection algorithm based on the Internet of things", Application of micro-computer, vol,27, no. 9, **(2011)**, pp.20-26.

Authors

Xiaolin Liang, He now studies in College of Information Science and Engineering and is a Ph. D. candidate in Ocean University of China. His research interests include ultra-wideband radio systems, 60GHz wireless communication system.

Tingting Lv, She received the Ph. D. degree in College of Information Science and Engineering from Ocean University of China in 2013. She is now a lecture in College of Information Science and Engineering. Her research interests include ultra-wideband radio systems, 60GHz wireless communication system.

Hao Zhang, He received the MBA degree in New York Institute of Technology, American in 2001 and the Ph. D. degree in Electrical and Computer Engineering from the University of Victoria, Canada in 2004. He was a Project Manager for Microsoft Inc. in United States during January 2000-May 2000. During 2004-2008, he was the Vice President for the United States Gamma Capital Inc. He is now an Adjunct Assistant Professor in the Department of Electrical and Computer Engineering. Also he becomes a professor and the Ph. D. supervisor in College of Information Science and Engineering from Ocean University of China in 2006. His research concerns ultra-wideband radio systems, 60GHz wireless communication system and MIMO wireless communication.

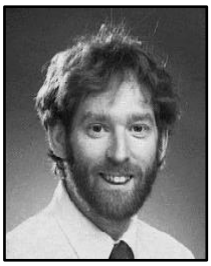

T. Aaron Gulliver, He received the Ph. D. degree in Electrical and Computer Engineering from the University of Victoria, Canada in 1989. He is now a professor and the Ph. D. supervisor in the Department of Electrical and Computer Engineering. In 2002, he becomes a Fellow of the Engineering Institute of Canada, and in 2012 a Fellow of the Canadian Academy of Engineering. He is also a senior member of IEEE. His research concerns information theory and communication theory, algebraic coding theory and smart grid and ultra-wideband communication.